J. Nat. Acad. Sci. ROK, Vol. 62, No. 1 (2023) 275-295

Nano-biomarker based surface-enhanced Raman spectroscopy for selective diagnosis of gallbladder and liver injury*

Sanghwa Lee[1], Eunyoung Tak[2], Yu Jeong Cho[3,4], Jiye Kim[2], Jooyoung Lee[2], Ryunjin Lee[2], Kwanhee Lee[2], Minsung Kwon[2], Young-In Yoon[5], Sung-Gyu Lee[5,6], Jung-Man Namgoong[4*] and Jun Ki Kim[1,2**]

담낭 및 간 손상의 선택적 진단을 위한 나노 바이오마커 기반의 표면 강화 라만 분광법*

이상화[1], 탁은영[2], 조유정[3,4], 김지예[2], 이주영[2], 이륜진[2], 이관희[2], 권민성[2], 윤영인[5], 이승규[5,6], 남궁정만[4*], 김준기[1,2**]

* The work was supported by the Research Grant 2022 of the National Academy of Sciences, Republic of Korea

** Sanghwa Lee, Eunyoung Tak, and Yu Jeong Cho have contributed equally to this work. Correspondence: Jung-Man Namgoong (namgoong2940@gmail.com) and Jun Ki Kim (kim@amc.seoul.kr)

[1] Biomedical Engineering Research Center, Asan Medical Center, Seoul 05505, Republic of Korea

[2] Department of Convergence Medicine, Asan Medical Center, University of Ulsan College of Medicine, Seoul 05505, Republic of Korea

[3] Department of Surgery, Hanyang University Guri Hospital, Hanyang University School of Medicine, Guri, 11923, Korea

[4] Department of Surgery, Asan Medical Center, University of Ulsan College of Medicine, Seoul,

Abstract

During living donor liver transplantation, a number of blood vessels and bile ducts are anastomosed while the liver and gallbladder are resected in the donor and recipient. It is necessary to detect and treat to complications after surgery early by evaluating the proper function of blood vessels and biliary tract. A biosensing chip that can monitor the patient's health status from the bile excreted during the recovery process has been developed using a surface-enhanced Raman sensing chip. Surface-enhanced Raman spectroscopy signals of bile obtained from normal, bile duct ligation (BDL), and gallbladder damage mouse models using a cautery device were identified and analyzed. The surface-enhanced Raman chip with a nanometer-level porous structure can selectively separate the nanometer biomarkers and measure the Raman signal. Through the detection of nanometer biomarkers in bile and comparative analysis of histopathology, the Raman signal in the damaged gallbladder was compared with that caused by BDL liver damage, showing that it becomes a biosensing chip for monitoring recovery.

Keywords : Bile duct ligation (BDL), Gallbladder cauterization, Surface enhanced Raman spectroscopy (SERS), Nano-biomarker, Principle component analysis (PCA)

초 록

생체 간이식을 하는 동안 여러 혈관과 담관을 문합하고 기증자와 수혜자의 간과 담낭을 절제합니다. 혈관과 담도의 적절한 기능을 평가하여 수술 후 합병증을 조기에 발견하고 치료하는 것이 필요합니다. 표면 강화 라만 센싱 칩을 이용해 회복 과정에서 배설된 담즙으로 환자의 건강 상태를 모니터링 할 수 있는 바이오 센싱 칩을 개발 하였습니다. 소작 장치를 사용하여 정상, 담관 결찰(BDL) 및 담낭 손상 마우스

05505, Korea
[5] Division of Liver Transplantation and Hepatobiliary Surgery, Department of Surgery, Asan Medical Center, University of Ulsan College of Medicine, Seoul, 05505, Korea
[6] Member, The National Academy of Sciences, Republic of Korea

모델에서 얻은 담즙의 표면 강화 라만 분광기 신호를 식별하고 분석 하였습니다. 나노미터 수준의 다공성 구조를 가진 표면 강화 라만 칩은 나노미터 바이오마커를 선택적으로 분리하고 라만 신호를 측정할 수 있습니다. 담즙에서 나노미터 바이오마커를 검출하고 조직병리학적 비교분석을 통해 손상된 담낭의 라만 신호와 BDL 간 손상으로 인한 라만 신호를 비교하여 환자의 회복을 모니터링하는 바이오센싱 칩으로서의 가능성을 보여주었습니다.

주제어: 담관 결찰술, 담낭소작술, 표면강화라만칩, 나노바이오마커, 주성분 분석

Statements and Declarations

The authors declare no conflict of interest.

Acknowledgements

This work was supported by the National Research Foundation of Korea (NRF) (2018R1D1A1B07048562, 2019R1A2C2084122, 2020R1A2C2102137) and MRC grant (2018R1A5A2020732) by the Ministry of Science & ICT (MSIT), by a grant of the Ministry of Trade, Industry, and Energy under Industrial Technology Innovation Program (20000843) and by Korea Health Technology R&D Project through the Korea Health Industry Development Institute (KHIDI), funded by the Ministry of Health & Welfare, Republic of Korea (HI18C2391). This study was also supported by a grant (2021IL0009, 2021IP0027) from the Asan Institute for Life Sciences, Asan Medical Center, Seoul, Korea.

목 차

Introduction

Living donor liver transplantation (LDLT) is the surgical process of the removal of diseased or malfunctioning liver and its replacement with a portion of healthy liver from a living donor. In the middle of LDLT, the recipient procedure of LDLT using a right lobe graft and surgery technique is used for the anastomosis of blood vessels, such as the hepatic artery, hepatic vein, portal vein, inferior vena cava, and bile duct [1]. If the patency of these blood vessels is not smooth after surgery, liver function deteriorates [2]. Therefore, to evaluate the proper function of blood vessels and the biliary tract, liver Doppler ultrasonography and vascular reconstruction computerized imaging should be performed at regular intervals to detect and treat complications early [3]. On the other hand, biliary tract complications, such as bile leakage around the biliary anastomosis or biliary narrowing, are common in liver transplantation [4, 5]. In the case of bile leakage, if it is properly drained through the drainage tube installed during surgery, the leakage of bile stops over time with ductal wound healing. In the case of biliary stenosis, it should be solved by widening the narrowed stenosis site by inserting a stent into the biliary tract as it can cause jaundice, pruritus, or liver failure [6]. The drainage of bile is usually performed by the installation of a drain tube in the biliary tract from the outside of the liver. Since a cauterizer is used to excise the biliary tract and blood vessels during organ transplantation surgery, heat damage can cause inflammation, which can become a burden on the patient [7]. In addition, as liver transplantation requires administration of immunosuppressants for a long time after surgery [8], the risk of infection is very high, especially in the early stages of transplantation [9]. As the patient is exposed to the risk of infection with a bile drainage tube after surgery, it is important to track the recovery of the biliary tract so that the drainage tube can be removed as soon as recovery of the biliary injury is confirmed.

To prevent complication-mediated liver malfunction, the diagnosis is usually made from biopsy of the tissue to determine the pathological inflammation of the existing organs and tissues [10]. However, tissue biopsy is invasive and biopsied samples do not guarantee representativeness. Though the occurrence of liver and biliary tract-related inflammation can be detected by measuring the levels of inflammatory cytokines, such as IL-2, TNF-α, and IL-18 from the blood [11], it is difficult to specify the inflamed organ. Therefore, it is necessary to find a novel, low-invasive, and precise biomarker that can identify the presence of bile duct injury.

Biomarkers that can be targeted *in vivo* are cells (~ tens of μm), erythrocytes (~8 μm), bacteria (~1 μm), viruses (~400 nm), exosomes (several nm to tens of nm depending on their size), proteins, or the smaller molecules, such as cell-free nucleic acids, which are likely to be distributed in body fluids, including a small amount in the blood and urine [12-14]. In fact, since there are several cases where various biomarkers are mixed in biological by-products, if nanometer biomarkers can be selectively detected, results with less noise can be obtained and the accuracy can be improved [15]. Therefore, the development of a device that can rapidly detect these factors is crucial.

Currently, the demand for high-sensitivity biosensors that can detect nano-molecules quickly and accurately is steadily increasing. One of the methods that can solve this demand is the Raman spectroscopy system, which is a spectroscopic analysis that measures the inelastic scattering of light particles of a laser that is incident on a biomarker. Organic and inorganic molecules have their own Raman shift spectrum; therefore, the Raman analysis is a useful measurement method for detecting chemical species in samples. Raman spectroscopy technology has the strongest application potential as a fingerprinting technology for diagnosing diseases in complex organisms, such as living organisms, with the advantage of having multiple detection and functionality of more than tens of multiple detections due to the narrow signal bandwidth. Recently, Raman measurement

at the single molecular scale has been reported to be possible with the surface-enhanced Raman method based on the nanostructure. In a previous study, a surface-enhanced Raman chip based on a nanorod array was fabricated and selectively enhanced Raman signals were obtained by filtering the nano biomarkers in urine [16].

In this study, a change in the Raman signal was measured by simulating the damage caused by the biliary obstruction that occurs during liver transplantation by manufacturing a bile duct ligation (BDL)-type animal model. In addition, the Raman signal of inflammation caused by heat damage during liver transplantation was measured through the cauterization of the gallbladder as shown in Figure 1. Through these results, we confirmed that a surface-enhanced Raman bio-sensing chip based on nano-biomarker detection that can monitor the patient's condition from bile excreted from liver transplant patients is possible.

Materials and Methods

Bile duct ligation

Anesthesia was induced by the inhalation of 4 vol% isoflurane, and maintained with 1.5-2.0 vol% isoflurane in 100% oxygen at a flow rate of 1 L/min. The liver was lifted with a moistened (0.9% NaCl solution) cotton swab, such that the ventral side of the liver stuck to the diaphragm and the hilum was clearly visible. The bile duct was exposed by caudal movement of the gut. A 5-0 silk suture was placed around the bile duct and secured with two surgical knots. A second cranial ligation was added in the same manner but did not dissect the bile duct in-between. A 0.9% NaCl solution was applied to the peritoneal cavity and the abdominal organs were replaced in their physiological positions. The peritoneum and skin were closed with a simple continuous suture with 5-0 silk, and the operation area was sterilized with betadine followed by 70% ethanol (two to three times) using cotton swabs. An intraperitoneal injection of tramadol 0.25 mg/kg was performed immediately after surgery.

Thermal cauterization treatment

The mice were anesthetized in the same manner as bile duct ligation and the abdomen was opened. The liver was moved with a wet cotton swab to reveal the gallbladder. The gallbladder was cauterized with high-temperature cautery (Change-A-Tip, Bovie, USA).

Blood sampling and laboratory tests

Whole blood samples were collected from the inferior vena cava of anesthetized mice. The collected blood was allowed to clot for 30 min at 24˚C and centrifuged at 2,500 x g for 20 min at 4˚C. To separate the serum from the clotted cells, the transparent upper phase was transferred

into new tubes. The serum AST and ALT levels were detected using an automated analyzer (Hitachi 7180, Tokyo, Japan).

Western blot

Protein lysates were obtained by homogenized liver tissues in RIPA buffer (Cat#89900, Thermo Fisher Scientific, US). Approximately 15 μg of liver tissue proteins were separated by 15% polyacrylamide gel electrophoresis and transferred to a nitrocellulose membrane for the subsequent steps. The membranes were blocked with 5% bovine serum albumin (Cat#82-100-6, Millipore Corporation, USA) in Tris-buffered saline-Tween-20 and then incubated with primary antibody. The levels of lipocalin-2 (Cat#ab63929, Abcam, UK) and vimentin (Cat#sc-6260, Santa Cruz Biotechnology, USA) were observed. Protein signals were detected by enhanced chemiluminescence (ECL; Cat#NCI34095, Thermo Fisher Scientific) system and captured using Luminograph II (Cat#WSE-6200, Atto, Japan). For the loading control, the blots were washed and re-probed for actin using HRP conjugated monoclonal β-actin antibody (A3854; Sigma-Aldrich, USA).

Histology analysis

The liver and gallbladder tissues from each group were fixed in 4% paraformaldehyde (pH 7.4; Sigma-Aldrich) and embedded in paraffin blocks. The paraffin blocks were sectioned into 4-μm-thick slides and the sections were deparaffinized, rehydrated, and stained with hematoxylin and eosin. The morphological changes to the liver tissues were observed using a light microscope (BX53 microscope with DP27 camera; Olympus corporation, Tokyo, Japan). For Sirius Red staining, the deparaffinized slides were incubated in Picro-Sirius Red Solution (Cat#ab150681, Abcam)

Statistical analyses

The data were analyzed using GraphPad Prism 5.0 software (GraphPad Software, La Jolla, CA, USA). Hepatic tissue injury scores have been described as medians and ranges. All the data have been described as mean ± standard deviation for ten samples per condition. Immunoblotting data were obtained from two procedures. Statistical one-way analysis of variance (ANOVA) with Bonferroni's correction was performed. A P-value < 0.05 was considered as statistically significant.

Surface-enhanced Raman Sensing chip preparation

For filtering the nanometer markers from bile and amplifying the Raman signal, a vertically aligned gold-ZnO nanorod-based surface-enhanced Raman chip, illustrated in Fig. 1, was fabricated. The ZnO nanostructure support was prepared in a hydrothermal method, and a solution was prepared by dissolving 10 mM zinc nitrate hexahydrate zinc nitrate hexahydrate and 0.9 mL ammonium hydroxide zinc nitrate hexahydrate (Sigma Aldrich Co., St. Louis, USA) in DI water. The ZnO nanorods were grown by dipping a Si wafer (LG SILTRON INC., KOREA) in this solution and maintaining it at 90°C for 50 minutes. The grown nanorods were 400-600 nm in length and 50 nm in diameter, and 200 nm thickness. Au was coated on these ZnO nanostructures using a thermal evaporator (Alpha Plus Co., Korea). A SERS chip was prepared by cutting a specimen of Au-ZnO nanorods on Si to a size of 0.5 × 0.5 mm.

Raman measurements and principal component analysis

The bile obtained from the animal model was placed on the SERS chip as a drop of 0.5 μL; additionally, 30 min later, the sample was loaded into a Raman spectroscopy system (FEX-INV, NOST, Korea) attached to a

microscope (IX-73, Olympus, Japan) and measurement was carried out.

A spectrum was obtained by irradiating a Raman 785 nm wavelength laser to the area where the nano biomarker diffused from the bile drop into the nanostructure. The Raman spectral spectrum was measured in units of 2.5 cm-1 for the 450 ~ 2100 cm-1 spectral region. Fifth order polynomial fitting was performed as a post-signal process, and it was diagrammed through Origin 2018 software. Data grouping was performed by statistical classification on Raman signals using the PCA method, and conducted using the XLSTAT 2019 software.

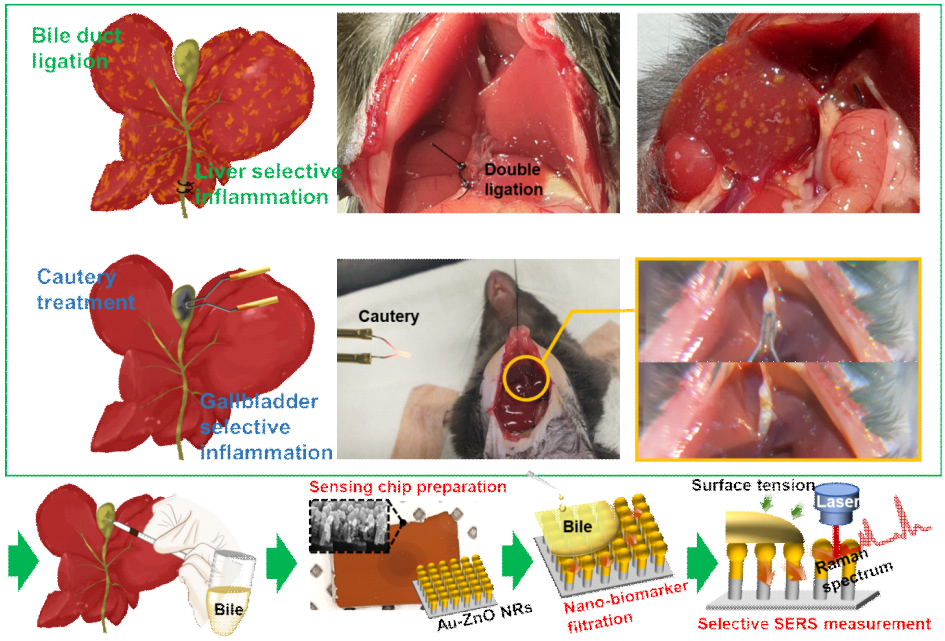

Fig. 1 Outline of animal model development and nanometer biomarker Raman measurement

Results and Discussion

Comparison of the effects of bile duct ligation and gallbladder cauterization on liver damage

The BDL animal model is a common method for imitating cholestasis, which represents a reduction or obstruction of bile flow [17]. Cholestasis is a frequent consequence of liver transplantation, and severe cholestasis can be associated with irreversible liver damage requiring re-transplantation [18]. In the BDL model, the duct that secretes bile from the gallbladder to the duodenum is blocked and the bile refluxes into the liver, resulting in cholestasis (Figure 1, Bile duct ligation).

On the other hand, liver transplantation is commonly accompanied by cholecystectomy (gallbladder ablation). Cholecystectomy is an operative procedure on the biliary tract, first described by Carl Langenbuch in 1882 [19]. During a cholecystectomy, the cystic duct and cystic artery are ligated and incised with electrical surgical cutting by the thermal effect of high-frequency cautery. During this procedure, the gallbladder is removed and the common bile duct is partly damaged by heat. To mimic these injuries in animal models, the current study created the following gallbladder thermal cauterization model (Figure 1, Cautery treatment).

As cholestasis is a well-known cause of liver injury with complex pathological cascades [20], pathological changes in the liver tissue were observed. The histological examination of the liver showed tissue necrosis and lymphatic infiltration in the liver parenchyma in BDL mice (Figure 2a). In addition, the total bilirubin, aspartate aminotransferase (AST), and alanine aminotransferase (ALT), the serum markers related to liver damage, were significantly elevated (Figure 2b). Lipocalin-2, a protein that reflects apoptosis in liver tissue, and vimentin, which stabilizes type I collagen and causes inflammation-related histological changes in the liver, were also significantly elevated (Figure 2c). However, with respect to

gallbladder cautery, the indicators related to liver tissue damage were not different from those of the normal liver tissue.

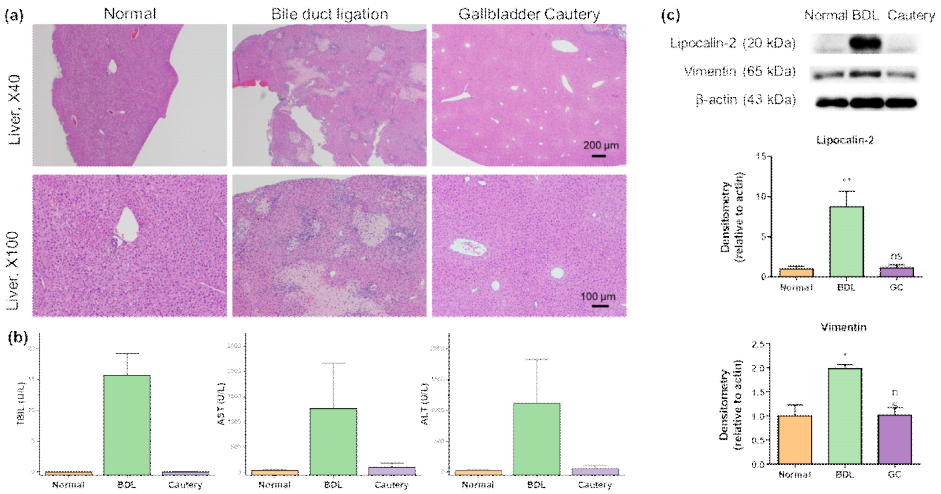

Fig. 2 Evaluation of liver damage and liver function impairment (a) Hematoxylin and Eosin (H&E) staining result of liver tissues from normal, bile duct ligation (BDL), and gallbladder cautery (Cautery) groups observed under ×40 or ×100 magnification. Scale bar, 200 μm and 100 μm for each magnification. (b) total bilirubin (U/L), AST (U/L), and ALT (U/L) levels were measured in the serum of each group. (c) Liver damage-related protein expression in the normal, BDL, and cautery groups with relative density. All expressions are normalized to β-actin and compared to the Normal group. *, $p < 0.05$; **, $p < 0.01$; ns, not significant

Assessment of gallbladder damage via histopathology

As the gallbladder is an organ that stores bile, the inside of the gallbladder is tightly surrounded by epithelial cells to protect from damage caused by bile acid. The epithelium forms mucosal folds, giving it elasticity. The lamina propria, located close to the epithelium, consists of loose connective tissue, through which veins and arterioles pass and lymphocytes migrate. Below the lamina propria lies the muscularis layer and the adventitia layer [21]. In the normal tissue sample, the epithelium surrounded the inside through the mucosal folds (Figure 3a). In the BDL tissue sample, most of the epithelium was intact while the mucosal folds were extended.

In the gallbladder cauterization tissue sample, the epithelium was partly lost (Figure 3a). Further investigation of the collagen connective tissue staining with Picro Sirius Red staining confirmed the epithelium surrounding the collagen connective tissue layer in the normal and BDL groups. However, in the gallbladder cauterization group, the collagen layer was completely exposed to the lumen. That is, protection of the gallbladder tissue after thermal cauterization is difficult by epithelial cells.

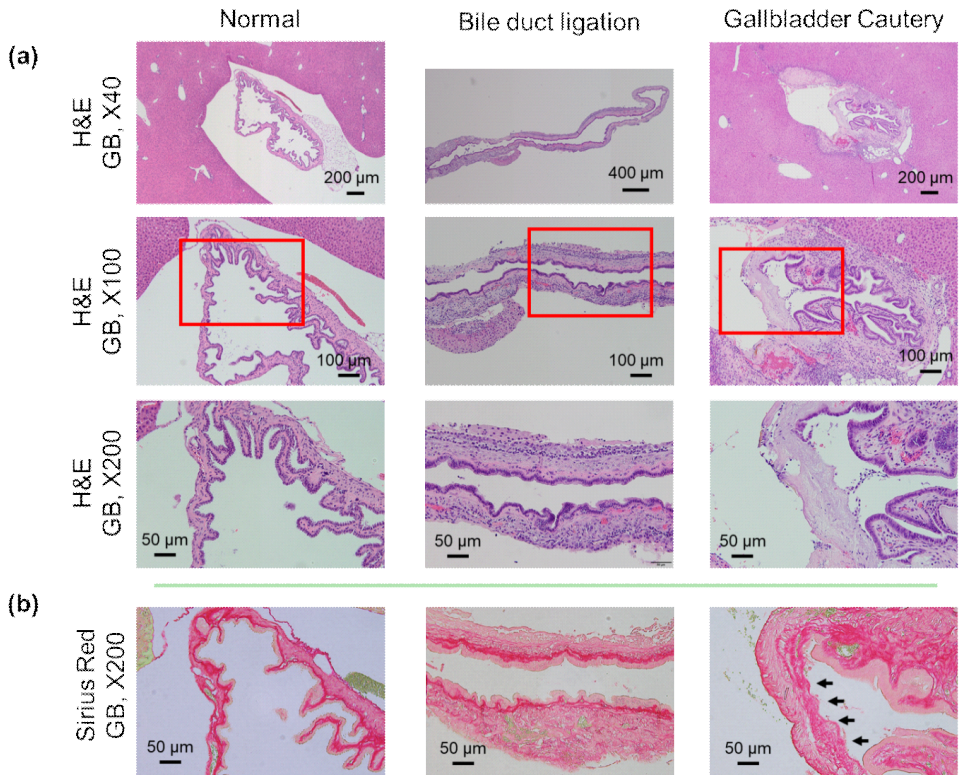

Fig. 3 Gallbladder damage evaluation (a) hematoxylin and eosin (H&E) staining result of the gallbladder and nearby liver tissue in normal, bile duct ligation (BDL), and gallbladder cautery (Cautery) group observed under ×40, ×100, and ×200 magnification with a scale bar. (b) Picro-Sirius Red staining result of the gallbladder in the normal, BDL, and cautery group under ×200 magnification. A serial section of the same sample used for H&E staining was stained and observed. The black arrows indicate the damaged inner epithelium of the gallbladder

Signal analysis through Raman spectra

The area diffused in the spherical direction from the bile dropped on the Au-ZnO-based surface-enhanced Raman spectroscopy (SERS) nanochip for nano-biomarker detection appears darker than the bare area. This area is a result of the nanometer biomarker being diffused into the nano-porous area. Subsequent to confirmation that the beam spot is located in this area by opening the laser front-shutter, Raman spectroscopic measurement was performed. The Raman signals of normal, BDL, and gallbladder (GB) cauterization were graphed as shown in Figure 4. The mean spectrum is plotted with solid lines, and the standard deviation is plotted with shades. In the case of normal and BDL, there was no specific peak or appearance of very small peak; however, in the case of GB cauterized bile, remarkable peaks appeared. Main peaks were observed at 881 cm^{-1} for tryptophan [22, 23], 912 cm^{-1} for glucose [23, 24], 1002 cm^{-1} [22, 25], 1033 cm^{-1} [22, 26], 1605 cm^{-1} for phenylalanine [23, 26], 1163 cm^{-1} for tyrosine [22, 23], 1242 cm^{-1} for amide III [23, 27], and 1374 cm^{-1} for nucleic acid [26, 28]. The assignment of each major peak and its reference are shown in Table 1. In particular, collagen-related assignment is seen in 1002, 1033, 1163, and 1242 cm^{-1}, and the correlation can be found with the GB cautery result in Figure 3. In hematoxylin and eosin (H&E) staining, the normal and BDL inner epithelial cells remain closed; however, in GB cautery, the inner epithelial cells remain open even a few days after the procedure at the heat injury site. In BDL, tensile strain is applied to the gallbladder to the extent that internal wrinkles disappear; however, the internal epithelial cells remain closed. Considering that more lymphatic cells were observed in the adventitia (or serosa) of the gallbladder of BDL mice than in that of normal mice (Figure 3a), inflammatory changes in the gallbladder are not reflected in the bile components. That is, if the gallbladder epithelium is intact, the inflammatory changes in the gallbladder and liver do not affect the SERS-measurable contents of the bile. Therefore, the presence

of internal epithelial cells is a major factor in determining the release of the nanometer markers contributing to Raman signals. This approach is also verified by the Sirius Red staining results, and as shown in Figure 3b, it can be seen that the Sirius Red is darkly stained in the area where collagen is highly distributed. In the normal and BDL cases, high-density collagen is closed by inner epithelial cells; however, in cautery cases, collagen regions are exposed to the lumen of the gallbladder. Therefore, it is presumed that damages in the internal epithelium caused by heat injury can cause the flow of collagen-related biomarkers into the bile. In addition, thermal injury can cause necrosis, which induces rupture of the cell membrane and nucleic envelope with DNA leakages [29]. During necrotic cell death, cell-consisting materials can be leaked into neighboring body fluids; in case of the gallbladder, the leaked fluid will probably be bile.

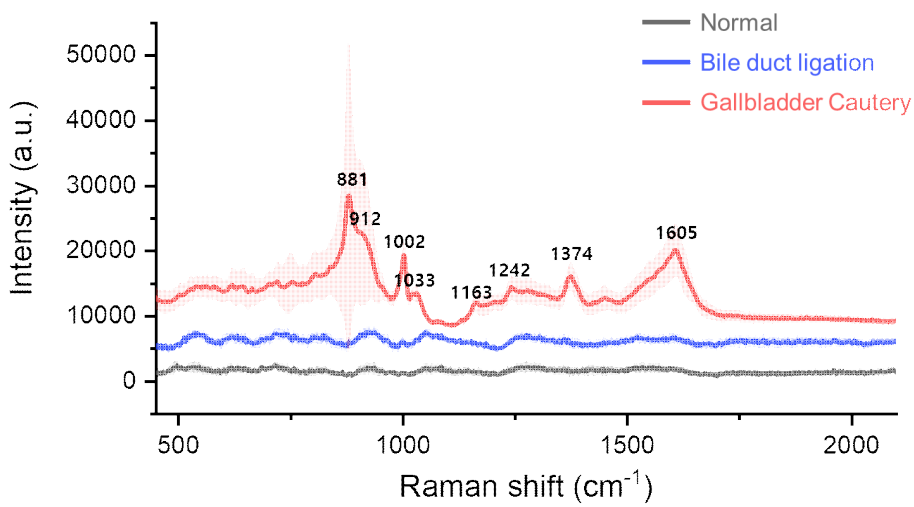

Fig. 4 Averaged Raman spectra in the normal (black line), BDL (blue line), and gallbladder cauterized (red line) animal models. The standard deviation in each Raman spectrum is the smear color, and the value for the main peak is expressed numerically

Table 1. Assignment of Raman peak in the GB cautery sample

Peak (cm^{-1})	Assignment	Ref.
881	Tryptophan	[22, 23]
912	Glucose	[23, 24]
1002	Phenylalanine(collagen assignment)	[22, 25]
1033	Phenylalanine(collagen assignment)	[22, 26]
1163	Tyrosine (collagen type I)	[22, 23]
1242	Amide III of collagen	[23, 27]
1374	Nucleic acid	[26, 28]
1605	Phenylalanine, tyrosine	[23, 26]

Principal component statistical analysis of results

The spectrum for the nanometer biomarkers of GB cautery consists of multiple variables (peaks), and monitoring through a single variable is required for sensing. Principal component analysis (PCA) is a statistical analysis of functions with an algorithm that reduces the variables [16, 30], and is a useful approach to minimize the variables obtained from this Raman spectrum. The PCA results of Raman spectra for normal, BDL, and GB cautery models are shown in Fig. 5a; additionally, the variability of PC1, PC2, and PC3 were 60.9%, 22.2%, and 3.4%, respectively. As shown in Figure 5b, the baseline that distinguishes injuries caused by cautery in the PC1 and PC2 planes is well determined. On the other hand, there was hardly any data distinction between the normal and BDL models. From the results of the Raman signal in the bile, it was shown that monitoring according to the source of damage occurring during liver transplantation is possible. Liver damage due to stenosis of the bile duct means that the biomarkers, such as total bilirubin (TBIL), AST, and ALT are monitored from the amount of release into the blood, and damage to the lining of the gallbladder (bile duct) due to thermal cauterization is monitored from the nano-biomarkers in the bile.

An excessive use of electrocautery to control biliary duct bleeding can clinically lead to early postoperative bile leak [31, 32]. Most biliary leaks occur within 1 to 3 months after liver transplantation and account for a significant portion of about 1-25% of the biliary complications of transplantations performed [33, 34]. We suggest that it may help reduce the morbidity and the hospitalization period if the damage to the bile duct caused by electrocautery can be detected quickly and conveniently using Raman spectroscopy. Furthermore, through additive studies, it is expected that it could be possible to quickly and easily monitor ischemia, which causes damage to the layer of the bile duct, anastomotic stricture caused by reperfusion injury, and biloma.

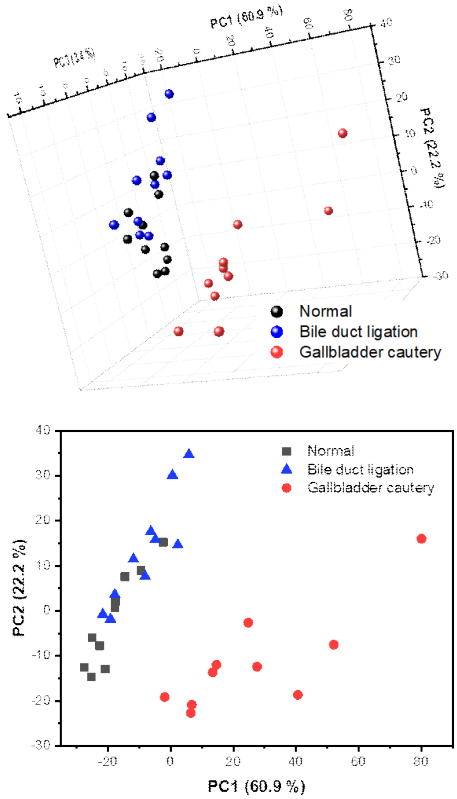

Fig. 5 (a) Analysis results up to the third principal component of normal, BDL, and gallbladder cauterization Raman results, (b) providing a baseline for distinguishing the gallbladder cauterization results in the PC1 and PC2 planes (green dashed line)

Conclusion

To monitor the recovery of the liver transplant-related patients, a biosensing chip that acquires surface-enhanced Raman signals from the biomarkers in excreted bile was developed. An animal model for monitoring the liver and gallbladder (bile duct) injury was provided, and biosensing Raman chip measurement was performed. Liver damage due to bile duct stenosis was induced using mouse BDL, and samples for selective damage to the gallbladder (bile duct) were prepared from gallbladder damage through cauterization. The liver function was evaluated through liver histopathology and blood TBIL, AST, and ALT; additionally, it was confirmed that the liver function was dramatically decreased in BDL mice. These results were verified by measuring the lipocalin-2 and vimentin levels in the liver tissue. On the other hand, it was confirmed through H/E staining of the gallbladder that the epithelium of the gallbladder disappeared only in the case of damage caused by heat cauterization. Moreover, through Sirius Red staining, it was confirmed that the collagen distribution was exposed to the inside of the gallbladder due to the disappearance of epithelium. Raman spectra were obtained for normal, BDL, and cautery samples; additionally, a remarkable peak appeared only in the case of gallbladder cauterization samples. Most of these peaks come from collagen-related sources, including phenylalanine, which are mainly found in bio-samples. This Raman signal assignment result is coherent with the result of exposure of the high density collagen region due to epithelium disappearance, as shown in Sirius Red staining. Through PCA, the criteria for sensing heat injury in the gallbladder were determines.

References

Ben-Ari, Z., Pappo, O.,Mor, E.: Intrahepatic cholestasis after liver transplantation, *Liver Transplant*. 2003;**9**:1005-1018.

Best, L. M., Leung, J., Freeman, S. C., Sutton, A. J., Cooper, N. J., et al.: Induction immunosuppression in adults undergoing liver transplantation: a network meta-analysis, *Cochrane Database Syst Rev*. 2020;**1**:CD013203.

Chan, J. W., Taylor, D. S., Zwerdling, T., Lane, S. M., Ihara, K., et al.: Micro-Raman spectroscopy detects individual neoplastic and normal hematopoietic cells, *Biophys J*. 2006;**90**:648-656.

Chang, J. H., Lee, I., Choi, M. G.,Han, S. W.: Current diagnosis and treatment of benign biliary strictures after living donor liver transplantation, *World J Gastroentero*. 2016;**22**:1593-1606.

Chauvin, K. L.,Oleary, J. P.: Langenbuch,Carl and the First Cholecystectomy, *Am Surgeon*. 1995;**61**:746-747.

Cheng, W. T., Liu, M. T., Liu, H. N.,Lin, S. Y.: Micro-Raman spectroscopy used to identify and grade human skin pilomatrixoma, *Microsc Res Techniq*. 2005;**68**: 75-79.

Citores, M. J., Lucena, J. L., de la Fuente, S.,Cuervas-Mons, V.: Serum biomarkers and risk of hepatocellular carcinoma recurrence after liver transplantation, *World J Hepatol*. 2019;**11**:50-64.

Dovbeshko, G. I., Gridina, N. Y., Kruglova, E. B.,Pashchuk, O. P.: FTIR spectroscopy studies of nucleic acid damage, *Talanta*. 2000;**53**:233-246.

Durand, F., Francoz, C., Asrani, S. K., Khemichian, S., Pham, T. A., et al.: Acute Kidney Injury After Liver Transplantation, *Transplantation*. 2018;**102**: 1636-1649.

Fang, C., Yan, S.,Zheng, S.: Bile Leakage after Liver Transplantation, *Open Med (Wars)*. 2017;**12**:424-429.

Frank, C. J., Mccreery, R. L.,Redd, D. C. B.: Raman-Spectroscopy of Normal and Diseased Human Breast Tissues, Anal Chem. 1995;**67**:777-783.

Georgiev, P., Jochum, W., Heinrich, S., Jang, J. H., Nocito, A., et al.: Characterization of time-related changes after experimental bile duct ligation, *Brit J Surg*. 2008;**95**:646-656.

Hampe T, Dogan A, Encke J, Mehrabi A, Schemmer P, Schmidt J, et al. Biliary

complications after liver transplantation. Clinical transplantation 2006;20:93-6.

Housset, C., Chretien, Y., Debray, D.,Chignard, N.: Functions of the Gallbladder, *Compr Physiol*. 2016;6:1549-1577.

Kleiner, D. E., Brunt, E. M., Van Natta, M., Behling, C., Contos, M. J., et al.: Design and validation of a histological scoring system for nonalcoholic fatty liver disease, *Hepatology*. 2005;**41**:1313-1321.

Kochhar, G., Parungao, J. M., Hanouneh, I. A.,Parsi, M. A.: Biliary complications following liver transplantation, *World J Gastroenterol*. 2013;**19**:2841-2846.

Krafft, C., Neudert, L., Simat, T.,Salzer, R.: Near infrared Raman spectra of human brain lipids, *Spectrochim Acta A Mol Biomol Spectrosc*. 2005;**61**:1529-1535.

Lee, S., Namgoong, J. M., Jue, M., Joung, Y., Ryu, C. M., et al.: Selective Detection of Nano-Sized Diagnostic Markers Using Au-ZnO Nanorod-Based Surface-Enhanced Raman Spectroscopy (SERS) in Ureteral Obstruction Models, *Int J Nanomed*. 2020;**15**:8121-8130.

Lewandowska, L., Malyszko, J.,Joanna Matuszkiewicz-Rowinska, J.: Urinary and Serum Biomarkers for Prediction of Acute Kidney Injury in Patients Undergoing Liver Transplantation, *Ann Transplant*. 2019;**24**:291-297.

Moini, M., Schilsky, M. L.,Tichy, E. M.: Review on immunosuppression in liver transplantation, *World J Hepatol*. 2015;7:1355-1368.

Movasaghi, Z., Rehman, S.,Rehman, I. U.: Raman spectroscopy of biological tissues, *Appl Spectrosc Rev*. 2007;**42**:493-541.

Moy, B. T.,Birk, J. W.: A Review on the Management of Biliary Complications after Orthotopic Liver Transplantation, *J Clin Transl Hepatol*. 2019;7:61-71.

Narayanaswamy, B., Gonde, C., Tredger, J. M., Hussain, M., Vergani, D., et al.: Serial circulating markers of inflammation in biliary atresia - Evolution of the post-operative inflammatory process, *Hepatology*. 2007;**46**:180-187.

Panikar, S. S., Banu, N., Haramati, J., Gutierrez-Silerio, G. Y., Bastidas-Ramirez, B. E., et al.: Anti-fouling SERS-based immunosensor for point-of-care detection of the B7-H6 tumor biomarker in cervical cancer patient serum, *Anal Chim Acta*. 2020;**1138**:110-122,

Pezzotti, G., Boffelli, M., Miyamori, D., Uemura, T., Marunaka, Y., et al.: Raman spectroscopy of human skin: looking for a quantitative algorithm to reliably estimate human age, *J Biomed Opt*. 2015;**20**.

Seiler, C. A.: The bile duct anastomosis in liver transplantation, *Digest Surg.* 1999;**16**: 102-106.

Tag, C. G., Sauer-Lehnen, S., Weiskirchen, S., Borkham-Kamphorst, E., Tolba, R. H., et al.: Bile Duct Ligation in Mice: Induction of Inflammatory Liver Injury and Fibrosis by Obstructive Cholestasis, *Jove-J Vis Exp.* 2015.

Thuluvath P, Pfau P, Kimmey M, Ginsberg G. Biliary complications after liver transplantation: the role of endoscopy. Endoscopy 2005;37:9:857-63.

Tung BY, Kimmey MB. Biliary complications of orthotopic liver transplantation. Digestive Diseases 1999;17:133-44.

Yao, F. Z., Coquery, J.,Le Cao, K. A.: Independent Principal Component Analysis for biologically meaningful dimension reduction of large biological data sets, *Bmc Bioinformatics.* 2012;13.

Yin, C., Zhu, Z. J., Wei, L., Sun, L. Y., Zhang, H. M., et al.: Risk factors for portal vein stenosis in pediatric liver transplantation, *Clin Transplant.* 2020;**34**: e13992.

Zoepf, T., Maldonado-Lopez, E. J., Hilgard, P., Dechene, A., Malago, M., et al.: Diagnosis of biliary strictures after liver transplantation: Which is the best tool? *World J Gastroentero.* 2005;**11**:2945-2948.

Zong, W. X.,Thompson, C. B.: Necrotic death as a cell fate, *Gene Dev.* 2006;**20**: 1-15.